Steel and Composite Structures, *Vol. 34, No. 1* (*2020*) *141-154*
DOI: https://doi.org/10.12989/scs.2020.34.1.141

Vibration of angle-ply laminated composite circular and annular plates

Kadir Mercan[1], Farzad Ebrahimi[2] and Ömer Civalek[*3]

[1]*kdeniz University, Engineering Faculty, Division of Mechanics, Antalya, Turkey*
[2]*Imam Khomeini International University, Mechanical Engineering Dept. Qazvin, Iran*
[3]*China Medical University, Research Center for Interneural Computing, Taichung-Taiwan*

(*Received July 7, 2019, Revised October 29, 2019, Accepted November 16, 2019*)

Abstract. In the present paper, free vibration analysis of angle-ply laminated composite annular and circular plates is performed by numerical methods. First-order shear deformation plate theory is used for kinematic relations. The related governing equations of motion are discretized via differential quadrature and discrete singular convolution methods. Frequency values are obtained for different lamina scheme, thickness-to-radius ratio, and mode numbers. The advantages and accuracy of these two methods are also tested in detail.

Keywords: laminated composites; annular plates; circular plate; discrete singular convolution

1. Introduction

Circular and annular plates are widely used as an essential structural component in many important engineering applications like aerospace, marine, automobile, rocket, components of pressure vessels, and petro-chemical industries. For different purposes and usage aim, they are made of different composite materials. Anisotropic, laminated, and functionally graded composites are well known material types in application areas. During the 50 years of engineering applications, material properties and new materials have also been taken into consideration for modeling. It is known that, laminated composite materials have been widely chosen in many engineering applications. High strength-to-weight ratio is the best for design. In the literature, some plate and shell theories have been used during the past years Qatu (2004), Soedel (2004), Reddy (2003), Civalek (2004), Bisadi *et al*. (2012), Akgoz and Civalek (2012, 2017). At first, mathematical model is derived via any plate theories. Secondly, it is required to solve these differential equations for mechanical model. Also, there are large numbers of numerical methods for solution of the governing equations (Leissa 1993), Tornabene *et al.* (2014), Civalek (1998). Plate and shell components are generally subjected to some dynamic loads or free motion. By this time, free vibration analysis of annular and circular plates has received great attention by design engineers. Su *et al*. (2014, 2015) applied numerical technique for vibration analysis of laminated sector and annular plates. Stability and vibration analysis of composite sector plates have been made by Sharma *et al*. (2005). Three-dimensional frequency response of thick laminated annular sector plates has been investigated by Malekzadeh (2009) via differential quadrature method. Tornabene *et al.* (2013, 2014, 2016) gave detailed formulation and solution of curved plates and shells. Strong form finite element method (FEM) formulation for plates has also been derived by Fantuzzi and Tornabene (2014). Civalek (2006a, b, 2007, 2008a, b, 2013a, b, 2017) presented discrete singular convolution (DSC) solution for vibration problems of shells and plates. Detailed unified formulation and solution for beams, plates, and shells have given by Wang *et al*. (2016a, b), Avcar (2015, 2019). Free vibration of functionally graded moderately thick annular sector plates has been made by Saidi *et al.* (2011) and Pang *et al*. (2017). Viswanathan *et al.* (2009) discussed free vibration of layered annular circular plate of variable thickness using spline function approximation. Kahare and Mittal (2016, 2017) presented some solutions of circular and annular plates via FEM. Arefi *et al.* (2018) have been supplied numerical solution for carbon nanotube reinforced (CNTR) cylindrical pressure under thermals effect. Effect of thermal gradients on stress/strain distributions in a thin circular symmetric plate was analyzed by Aleksandrova (2016). Hyperbolic shear deformation theory for bending, buckling, and free vibration of sandwich plates made of functionally graded materials (FGM) was adopted by Abdelaziz *et al.* (2017). Hamzehkolaei *et al.* (2011) presented a numerical solution for thermal effect on axisymmetric bending of functionally graded circular and annular plates using differential quadrature method (DQM). Thermal stresses and deflections of functionally graded sandwich plates using a new refined hyperbolic shear deformation theory have been investigated by Bouchafa *et al.* (2015). Bouderba *et al.* (2016) analyzed the thermal stability of functionally graded sandwich plates using a simple shear deformation theory. Benchohra *et al.* (2018) also gave a detailed solution for functionally graded plates via new quasi-3D sinusoidal shear deformation theory. Natural vibration characteristics of a clamped circular plate in contact with fluid have been

*Corresponding author, Professor
E-mail: civalek@yahoo.com

ISSN: 1229-9367 (Print), 1598-6233 (Online)

solved by Jhung *et al.* (2005) and Azimi (1988). Tahouneh (2014) presented some numerical solution for free vibration analysis of bi-directional functionally graded annular plates resting on elastic foundations. Yousefzadeh *et al.* (2018) examined the dynamic response of functionally graded annular/circular plate in contact with bounded fluid under harmonic load. Quasi-3D static analysis of two-directional functionally graded circular plates was solved by Wu and Yu (2018). Also, state space meshless method for the 3D analysis of FGM axisymmetric circular plates has been applied by Wu and Yu (2016). Civalek and Demir (2011, 2016) and Demir and Civalek (2017) used numerical methods for nano modeling.

In this manuscript, free vibration analysis of laminated composite circular plate is performed via differential quadrature (DQ) and discrete singular convolution (DSC). The related governing equations of motion for circular plate are obtained via conical shell equations. Effects of different lay-up on frequencies of circular and annular laminated plates are discussed. Also, performance of DSC method is investigated in detail.

2. Solution methodology

Two different methods are used for solution. Firstly, differential quadrature is used. In DQ, differential equation transforms into a set of analogous algebraic equations as below

$$\left.\frac{\partial^r u}{\partial x^r}\right|_{x=x_i} = \sum_{k=1}^{N_x} A_{ik}^{(r)}\, u(x_k, y_j); \qquad r = 1,2,.....,N_x - 1 \tag{1}$$

$$\left.\frac{\partial^s u}{\partial y^s}\right|_{y=y_j} = \sum_{k=1}^{N_x} B_{jk}^{(s)}\, u(x_i, y_k); \qquad s = 1,2,.....,N_y - 1 \tag{2}$$

$$\left.\frac{\partial^{(r+s)} u}{\partial x^r \partial y^s}\right|_{x_i y_j} = \frac{\partial^r}{\partial x^r}\left(\frac{\partial^s u}{\partial y^s}\right)_{x_i y_j} = \sum_{k=1}^{N_x} A_{ik}^{(r)} . \sum_{m=1}^{N_y} B_{jm}^{(s)} u(x_k, y_m) \tag{3}$$

The second, third, and fourth-order derivatives are calculated via

$$B_{ij} = \sum_{k=1}^{N} A_{ik} A_{kj}, \quad C_{ij} = \sum_{k=1}^{N} A_{ik} B_{kj}, D_{ij} = \sum_{k=1}^{N} A_{ik} C_{kj} \tag{4}$$

Discrete singular convolution (DSC) is suggested by Wei (2001a, b) for the first time in order to fast solution of the mathematical physics problems (Wang *et al.* 2012, Civalek and Akgoz 2013, Gürses *et al.* 2012, Civalek and Acar 2007, Demir *et al.* 2016, Civalek *et al.* 2016, Hou *et al.* 2005, Civalek *et al.* 2010, Mercan and Civalek 2017). As similar the other discrete numerical methods, the function $f(x)$ and its derivatives with respect to x coordinate at a grid point x_i are approximated by a linear sum of discrete values $f(x_k)$ in a narrow bandwidth $[x\text{-}x_M, x\text{+}x_M]$ in DSC. Namely

$$\left.\frac{d^n f(x)}{d x^n}\right|_{x=x_i} = f^{(n)}(x) \approx \sum_{k=-M}^{M} \delta_{\Delta,\sigma}^{(n)}(x_i - x_k) f(x_k) \tag{5}$$

In this paper, the detailed formulation and mathematical details of the DQ and DSC methods are not given; interested readers may refer to the works of (Wei *et al.* 2001, Wei *et al.* 2002a, Wei *et al.* 2002b, Gürses *et al.* 2009, Baltacioglu *et al.* 2010, Baltacioglu *et al.* 2011, Civalek 2008, Civalek 2013, Duan *et al.* 2014, Civalek and Akgoz 2011, Mercan and Civalek 2016). It is mentioned that the use of the regularized Shannon kernel (RSK) is very effective. This kernel is as follows

$$\delta_{\Delta,\sigma}(x - x_k) = \frac{\sin[(\pi/\Delta)(x - x_k)]}{(\pi/\Delta)(x - x_k)} \exp\left[-\frac{(x - x_k)^2}{2\sigma^2}\right] \tag{6}$$

The solution is also made by DQM (Striz *et al.* 1995, Shu and Xue 1997, Civalek 2004). Detailed formulations for DQ and HDQ can be found in open literature.

3. Formulations

Consider a thick laminated circular plate as shown in Fig. 1.

After using the only normal and rotary inertia (I_1 and I_3), terms, governing differential equations of motion via FSDT can be given as

$$\begin{aligned}
&A_{11}\frac{\partial^2 u}{\partial x^2} + \frac{A_{11}}{R(x)}\sin\alpha\frac{\partial u}{\partial x} - \frac{A_{22}}{R^2(x)}\sin^2\alpha\cdot u + \frac{A_{33}}{R^2(x)}\frac{\partial^2 u}{\partial s^2} + \frac{(A_{12}+A_{33})}{R(x)}\frac{\partial^2 v}{\partial x \partial s}\\
&-\frac{(A_{22}+A_{33})}{R^2(x)}\sin\alpha\frac{\partial v}{\partial s} + \frac{A_{12}}{R(x)}\cos\alpha\frac{\partial w}{\partial x} - \frac{A_{22}}{R^2(x)}\sin\alpha\cdot\cos\alpha\cdot w - B_{11}\frac{\partial^2 \varphi_x}{\partial x^2}\\
&+\frac{B_{11}}{R(x)}\sin\alpha\frac{\partial \varphi_x}{\partial x} - \frac{B_{22}}{R^2(x)}\sin^2\alpha\cdot\varphi_x + \frac{B_{33}}{R^2(x)}\frac{\partial^2 \varphi_x}{\partial s^2}\\
&+\frac{(B_{12}+B_{33})}{R(x)}\frac{\partial^2 \varphi_s}{\partial x \partial s} - \frac{(B_{22}+B_{33})}{R^2(x)}\frac{\partial \varphi_s}{\partial s}\sin\alpha = I_1\frac{\partial^2 u}{\partial t^2}
\end{aligned} \tag{7}$$

$$\begin{aligned}
&\frac{(A_{12}+A_{33})}{R(x)}\frac{\partial^2 u}{\partial x \partial s} + \frac{(A_{22}+A_{33})}{R^2(x)}\sin\alpha\frac{\partial u}{\partial s} + A_{33}\frac{\partial^2 v}{\partial x^2} + A_{33}\frac{\sin\alpha}{R(x)}\frac{\partial v}{\partial x}\\
&-\frac{A_{33}}{R^2(x)}\sin^2\alpha\cdot v + \frac{A_{22}}{R^2(x)}\frac{\partial^2 v}{\partial s^2} - \frac{A_{44}}{R^2(x)}\cos^2\alpha\cdot v + \frac{(A_{22}+A_{44})}{R^2(x)}\cos\alpha\frac{\partial w}{\partial s}\\
&+\frac{(B_{12}+B_{33})}{R(x)}\frac{\partial^2 \varphi_x}{\partial x \partial s} + \frac{(B_{22}+B_{33})}{R^2(x)}\sin\alpha\frac{\partial \varphi_x}{\partial s} + B_{33}\frac{\partial^2 \varphi_s}{\partial x^2} + B_{33}\frac{\sin\alpha}{R(x)}\frac{\partial \varphi_s}{\partial x}\\
&-\frac{B_{33}}{R^2(x)}\sin^2\alpha\cdot\varphi_s + \frac{B_{22}}{R^2(x)}\frac{\partial^2 \varphi_s}{\partial s^2} + A_{44}\frac{\cos\alpha}{R(x)}\cdot\varphi_s = I_1\frac{\partial^2 v}{\partial t^2}
\end{aligned} \tag{8}$$

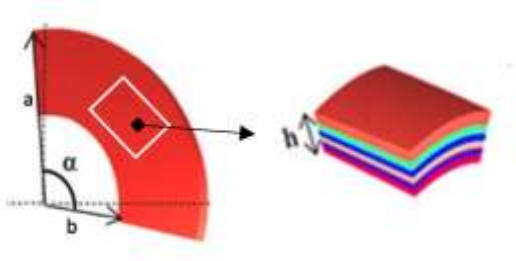

Fig. 1 Geometry and notation of an annular plate

$$-\frac{A_{12}}{R(x)}\cos\alpha\frac{\partial u}{\partial x}-\frac{A_{22}}{R^2(x)}\cdot u\cdot\sin\alpha\cdot\cos\alpha-\frac{(A_{22}+A_{44})}{R^2(x)}\cdot\cos\alpha\frac{\partial v}{\partial s}+A_{55}\frac{\partial^2 w}{\partial x^2}$$
$$+\frac{A_{55}}{R(x)}\sin\alpha\cdot\frac{\partial w}{\partial s}+\frac{A_{44}}{R^2(x)}\frac{\partial^2 w}{\partial s^2}-\frac{A_{22}}{R^2(x)}\cdot w\cdot\cos^2\alpha+A_{55}\frac{\partial\varphi_x}{\partial x}-\frac{B_{12}}{R(x)}\cos\alpha\cdot\frac{\partial\varphi_x}{\partial x}$$
$$+\frac{A_{55}}{R(x)}\sin\alpha\cdot\varphi_x-\frac{B_{22}}{R^2(x)}\sin\alpha\cdot\cos\alpha\cdot\varphi_x+\frac{A_{44}}{R(x)}\cdot\frac{\partial\varphi_s}{\partial s} \quad (9)$$
$$-\frac{B_{22}}{R^2(x)}\cdot\cos\alpha\frac{\partial\varphi_s}{\partial s}=I_1\frac{\partial^2 w}{\partial t^2}$$

$$B_{11}\frac{\partial^2 u}{\partial x^2}+\frac{B_{11}}{R(x)}\sin\alpha\frac{\partial u}{\partial x}-\frac{B_{22}}{R^2(x)}\cdot u\cdot\sin^2\alpha+\frac{B_{33}}{R^2(x)}\frac{\partial^2 u}{\partial s^2}+\frac{(B_{12}+B_{33})}{R(x)}\frac{\partial^2 v}{\partial x\partial s}$$
$$-\frac{(B_{22}+B_{33})}{R^2(x)}\sin\alpha\frac{\partial v}{\partial s}-A_{55}\frac{\partial w}{\partial x}+B_{12}\frac{\cos\alpha}{R(x)}\frac{\partial w}{\partial x}-\frac{B_{22}}{R^2(x)}\cdot w\cdot\sin\alpha\cos\alpha$$
$$+D_{11}\frac{\partial^2\varphi_x}{\partial x^2}+D_{11}\frac{\sin\alpha}{R(x)}\frac{\partial\varphi_x}{\partial x}-\frac{D_{22}}{R^2(x)}\varphi_x\sin^2\alpha+\frac{D_{33}}{R^2(x)}\frac{\partial^2\varphi_x}{\partial s^2}-A_{55}\varphi_x \quad (10)$$
$$+\frac{(D_{12}+D_{33})}{R(x)}\frac{\partial^2\varphi_s}{\partial x\partial s}-\frac{(D_{22}+D_{33})}{R^2(x)}\frac{\partial\varphi_s}{\partial s}\sin\alpha=I_3\frac{\partial^2\varphi_x}{\partial t^2}$$

$$\frac{(B_{12}+B_{33})}{R(x)}\frac{\partial^2 u}{\partial x\partial s}+\frac{(B_{22}+B_{33})}{R^2(x)}\frac{\partial u}{\partial s}\sin\alpha+B_{33}\frac{\partial^2 v}{\partial x^2}+B_{33}\frac{\sin\alpha}{R(x)}\frac{\partial v}{\partial x}$$
$$-B_{33}\frac{\sin^2\alpha}{R^2(x)}\cdot v+\frac{B_{22}}{R^2(x)}\frac{\partial^2 v}{\partial s^2}+\frac{A_{44}}{R(x)}\cdot v\cdot\cos\alpha-\frac{A_{44}}{R(x)}\frac{\partial w}{\partial s}+\frac{B_{22}}{R^2(x)}\cos\alpha\frac{\partial w}{\partial s}$$
$$+\frac{(D_{12}+D_{33})}{R(x)}\frac{\partial^2\varphi_x}{\partial x\partial s}+\frac{(D_{22}+D_{33})}{R^2(x)}\sin\alpha\frac{\partial\varphi_x}{\partial s}-D_{33}\frac{\partial^2\varphi_s}{\partial x^2} \quad (11)$$
$$+D_{33}\frac{\sin\alpha}{R(x)}\frac{\partial\varphi_s}{\partial x}-\frac{D_{33}}{R^2(x)}\sin^2\alpha\cdot\varphi_s+\frac{D_{22}}{R^2(x)}\frac{\partial^2\varphi_s}{\partial s^2}-A_{44}\cdot\varphi_s=I_3\frac{\partial^2\varphi_s}{\partial t^2}$$

For modal analysis, the below harmonic functions can be used

$$\begin{Bmatrix}u(x,s,t)\\v(x,s,t)\\w(x,s,t)\\\varphi_x(x,s,t)\\\varphi_s(x,s,t)\end{Bmatrix}=e^{i\omega t}\begin{Bmatrix}U(x,s,t)\\V(x,s,t)\\W(x,s,t)\\\Psi_x(x,s,t)\\\Psi_s(x,s,t))\end{Bmatrix} \quad (12)$$

If Eq. (12) is written in Eqs. (7)-(11), the final governing equations can be expressed as matrix form (Viswanathan *et al.*2015, Mehditabar *et al.* 2018)

$$L_{11}+L_{12}+L_{13}+L_{14}+L_{15}-\rho h\cdot\omega^2=0 \quad (13a)$$

$$L_{21}+L_{22}+L_{23}+L_{24}+L_{25}-\rho h\cdot\omega^2=0 \quad (13b)$$

$$L_{31}\cdot U+L_{32}\cdot V+L_{33}\cdot W+L_{34}\cdot\Phi_x+L_{35}\cdot\Phi_y-\rho h\cdot\omega^2=0 \quad (13c)$$

$$L_{41}\cdot U+L_{42}\cdot V+L_{43}\cdot W+L_{44}\cdot\Phi_x+L_{45}\cdot\Phi_y-\rho h^3\cdot\omega^2/12=0 \quad (13d)$$

$$L_{51}\cdot U+L_{52}\cdot V+L_{53}\cdot W+L_{54}\cdot\Phi_x+L_{55}\cdot\Phi_y-\rho h^3\cdot\omega^2/12=0 \quad (13e)$$

Differential operators in Eqs. (13(a))-(13(e)) are listed in Appendix.

4. Numerical solution of equation of motion

After adopted DSC method, the equations of motion of plate can also be written as (Viswanathan *et al.* 2015, Mehditabar *et al.* 2018)

$$^{DSC}L_{11}\cdot U+{}^{DSC}L_{12}\cdot V+{}^{DSC}L_{13}\cdot W+{}^{DSC}L_{14}\cdot\Phi_x+{}^{DSC}L_{15}\cdot\Phi_y-\rho h\cdot\omega^2=0$$
$$^{DSC}L_{21}\cdot U+{}^{DSC}L_{22}\cdot V+{}^{DSC}L_{23}\cdot W+{}^{DSC}L_{24}\cdot\Phi_x+{}^{DSC}L_{25}\cdot\Phi_y-\rho h\cdot\omega^2=0$$
$$^{DSC}L_{31}\cdot U+{}^{DSC}L_{32}\cdot V+{}^{DSC}L_{33}\cdot W+{}^{DSC}L_{34}\cdot\Phi_x+{}^{DSC}L_{35}\cdot\Phi_y-\rho h\cdot\omega^2=0 \quad (14)$$
$$^{DSC}L_{41}\cdot U+{}^{DSC}L_{42}\cdot V+{}^{DSC}L_{43}\cdot W+{}^{DSC}L_{44}\cdot\Phi_x+{}^{DSC}L_{45}\cdot\Phi_y-\rho h^3\cdot\omega^2/12=0$$
$$^{DSC}L_{51}\cdot U+{}^{DSC}L_{52}\cdot V+{}^{DSC}L_{53}\cdot W+{}^{DSC}L_{54}\cdot\Phi_x+{}^{DSC}L_{55}\cdot\Phi_y-\rho h^3\cdot\omega^2/12=0$$

Discrete form of these differential operators are as

$$^{DSC}L_{11}=A_{11}\cdot\Xi_x^{(2)}+\frac{A_{11}}{R(x)}\sin\alpha\cdot\Xi_x^{(1)}-\frac{A_{22}}{R^2(x)}\cdot U(i)\cdot\sin^2\alpha+\frac{A_{33}}{R^2(x)}\cdot\Xi_s^{(2)} \quad (15)$$

$$^{DSC}L_{12}=\frac{(A_{12}+A_{33})}{R(x)}\sin\alpha\cdot\Xi_{xs}^{(2)}\frac{\partial^2 V}{\partial x\partial s}-\frac{(A_{22}+A_{33})}{R^2(x)}\sin\alpha\cdot\Xi_s^{(1)} \quad (16)$$

$$^{DSC}L_{13}=\frac{A_{12}}{R(x)}\cos\alpha\cdot\Xi_x^{(1)}-\frac{A_{22}}{R^2(x)}\cdot W(i)\cdot\sin\alpha\cdot\cos\alpha \quad (17)$$

$$^{DSC}L_{14}=B_{11}\cdot\Xi_x^{(2)}+\frac{B_{11}}{R(x)}\sin\alpha\cdot\Xi_x^{(1)}-\frac{B_{22}}{R^2(x)}\cdot\Psi_x(i)\sin^2\alpha+\frac{B_{33}}{R^2(x)}\cdot\Xi_s^{(2)} \quad (18)$$

$$^{DSC}L_{15}=\frac{(B_{12}+B_{33})}{R(x)}\cdot\Xi_x^{(1)}\cdot\Xi_s^{(1)}-\frac{(B_{22}+B_{33})}{R^2(x)}\cdot\Xi_s^{(1)}\cdot\sin\alpha \quad (19)$$

$$^{DSC}L_{21}=\frac{(A_{12}+A_{33})}{R(x)}\cdot\Xi_x^{(1)}\cdot\Xi_s^{(1)}+\frac{(A_{22}+A_{33})}{R^2(x)}\sin\alpha\cdot\Xi_s^{(1)} \quad (20)$$

$$^{DSC}L_{22}=A_{33}\Xi_x^{(2)}+A_{33}\frac{\sin\alpha}{R(x)}\Xi_s^{(1)}$$
$$-\frac{A_{33}}{R^2(x)}\cdot V(i)\cdot\sin^2\alpha+\frac{A_{22}}{R^2(x)}\Xi_s^{(2)}-\frac{A_{44}}{R^2(x)}\cdot V(i)\cdot\cos^2\alpha \quad (21)$$

$$^{DSC}L_{23}=\frac{(A_{22}+A_{44})}{R^2(x)}\cdot\cos\alpha\cdot\Xi_s^{(1)} \quad (22)$$

$$^{DSC}L_{24}=\frac{(B_{12}+B_{33})}{R(x)}\cdot\Xi_x^{(1)}\cdot\Xi_s^{(1)}+\frac{(B_{22}+B_{33})}{R^2(x)}\sin\alpha\cdot\Xi_s^{(1)} \quad (23)$$

$$^{DSC}L_{25}=B_{33}\cdot\Xi_x^{(2)}+B_{33}\frac{\sin\alpha}{R(x)}\cdot\Xi_x^{(1)}$$
$$-\frac{B_{33}}{R^2(x)}\cdot\Psi_s(i)\cdot\sin^2\alpha+\frac{B_{22}}{R^2(x)}\cdot\Xi_s^{(2)}+A_{44}\cdot\frac{\cos\alpha}{R(x)}\cdot\Psi_s(i) \quad (24)$$

$$^{DSC}L_{31}=-\frac{A_{12}}{R(x)}\cos\alpha\cdot\Xi_x^{(1)}-\frac{A_{22}}{R^2(x)}\cdot U(i)\cdot\sin\alpha\cdot\cos\alpha \quad (25)$$

$$^{DSC}L_{32}=-\frac{(A_{22}+A_{44})}{R^2(x)}\cos\alpha\cdot\Xi_s^{(1)} \quad (26)$$

$$^{DSC}L_{33} = A_{55}\cdot\Xi_x^{(2)} + \frac{A_{55}}{R(x)}\sin\alpha\cdot\Xi_s^{(1)} + \frac{A_{44}}{R^2(x)}\cdot\Xi_s^{(2)} - \frac{A_{22}}{R^2(x)}\cdot W(i)\cdot\cos^2\alpha$$

$$^{DSC}L_{34} = A_{55}\cdot\Xi_x^{(1)} - \frac{B_{12}}{R(x)}\cos\alpha\cdot\Xi_x^{(1)} \tag{27}$$

$$+\frac{A_{55}}{R(x)}\cdot\Psi_x(i)\cdot\sin\alpha - \frac{B_{22}}{R^2(x)}\cdot\Psi_x(i)\cdot\sin\alpha\cdot\cos\alpha \tag{28}$$

$$^{DSC}L_{35} = \frac{A_{44}}{R(x)}\cdot\Xi_s^{(1)} - \frac{B_{22}}{R^2(x)}\cdot\cos\alpha\cdot\Xi_s^{(1)} \tag{29}$$

$$^{DSC}L_{41} = B_{11}\cdot\Xi_x^{(2)} + \frac{B_{11}}{R(x)}\sin\alpha\cdot\Xi_x^{(1)} - \frac{B_{22}}{R^2(x)}\cdot U(i)\cdot\sin^2\alpha + \frac{B_{33}}{R^2(x)}\cdot\Xi_s^{(2)} \tag{30}$$

$$^{DSC}L_{42} = \frac{(B_{12}+B_{33})}{R(x)}\cdot\Xi_x^{(1)}\cdot\Xi_s^{(1)} - \frac{(B_{22}+B_{33})}{R^2(x)}\sin\alpha\cdot\Xi_s^{(1)} \tag{31}$$

$$^{DSC}L_{43} = -A_{55}\cdot\Xi_x^{(1)} + B_{12}\frac{\cos\alpha}{R(x)}\cdot\Xi_x^{(1)} - \frac{B_{22}}{R^2(x)}\cdot W(i)\cdot\sin\alpha\cos\alpha \tag{32}$$

$$^{DSC}L_{44} = D_{11}\cdot\Xi_x^{(2)} + D_{11}\frac{\sin\alpha}{R(x)}\cdot\Xi_x^{(1)} - \frac{D_{22}}{R^2(x)}\sin^2\alpha + \frac{D_{33}}{R^2(x)}\cdot\Xi_s^{(2)} - A_{55}\cdot\Psi_x(i) \tag{33}$$

$$^{DSC}L_{45} = \frac{(D_{12}+D_{33})}{R(x)}\cdot\Xi_x^{(1)}\cdot\Xi_s^{(1)} - \frac{(D_{22}+D_{33})}{R^2(x)}\cdot\Xi_s^{(1)}\sin\alpha \tag{34}$$

$$^{DSC}L_{51} = \frac{(B_{12}+B_{33})}{R(x)}\cdot\Xi_x^{(1)}\cdot\Xi_s^{(1)} + \frac{(B_{22}+B_{33})}{R^2(x)}\cdot\Xi_s^{(1)}\sin\alpha \tag{35}$$

$$^{DSC}L_{52} = B_{33}\cdot\Xi_x^{(2)} + B_{33}\frac{\sin\alpha}{R(x)}\cdot\Xi_x^{(1)}$$
$$-B_{33}\cdot\frac{\sin^2\alpha}{R^2(x)}\cdot V(i) + \frac{B_{22}}{R^2(x)}\cdot\Xi_s^{(2)} + \frac{A_{44}}{R(x)}\cdot\cdot V(i)\cdot\cos\alpha \tag{36}$$

$$^{DSC}L_{53} = -\frac{A_{44}}{R(x)}\cdot\Xi_s^{(1)} + \frac{B_{22}}{R^2(x)}\cos\alpha\cdot\Xi_s^{(1)} \tag{37}$$

$$^{DSC}L_{54} = \frac{(D_{12}+D_{33})}{R(x)}\cdot\Xi_x^{(1)}\cdot\Xi_s^{(1)} + \frac{(D_{22}+D_{33})}{R^2(x)}\sin\alpha\cdot\Xi_s^{(1)} \tag{38}$$

$$^{DSC}L_{55} = D_{33}\cdot\Xi_x^{(1)} + D_{33}\frac{\sin\alpha}{R(x)}\cdot\Xi_x^{(1)}$$
$$-\frac{D_{33}}{R^2(x)}\cdot\Psi_s(i)\cdot\sin^2\alpha + \frac{D_{22}}{R^2(x)}\cdot\Xi_s^{(2)} - A_{44}\cdot\Psi_s(i) \tag{39}$$

DSC operator are given as

$$\Xi_x^n(\,) = \frac{\partial^{(n)}(\,)}{\partial x^{(n)}} = \sum_{k=-M}^{M}\delta_{\Delta,\sigma}^{(n)}(k\cdot\Delta x)(\,)_{i+k,j} \tag{40}$$

$$\Xi_s^n(\,) = \frac{\partial^{(n)}(\,)}{\partial s^{(n)}} = \sum_{k=-M}^{M}\delta_{\Delta,\sigma}^{(n)}(k\cdot\Delta s)(\,)_{i,j+k} \tag{41}$$

$$\Xi_x^1\Xi_s^{(n-1)}(\,) = \sum_{k=-M}^{M}\delta_{\Delta,\sigma}^{(1)}(k\cdot\Delta x)(\,)_{i+k,j}\sum_{k=-M}^{M}\delta_{\Delta,\sigma}^{(n-1)}(k\cdot\Delta s)(\,)_{i,k+j} \tag{42}$$

$$\Xi_x^{(n-1)}\Xi_s^1(\,) = \sum_{k=-M}^{M}\delta_{\Delta,\sigma}^{(n-1)}(k\cdot\Delta x)(\,)_{i+k,j}\sum_{k=-M}^{M}\delta_{\Delta,\sigma}^{(1)}(k\cdot\Delta s)(\,)_{i,k+j} \tag{43}$$

Similarly, coefficients related partial derivations in DQM can also be written as

$$\Xi_x^n(*) = \frac{\partial^{(n)}(*)}{\partial x^{(n)}} = \sum_{k=1}^{N}C_{i+k,j}^{(n)}(i)(*)_{i+k,j} \tag{44}$$

$$\Xi_s^n(*) = \frac{\partial^{(n)}(*)}{\partial s^{(n)}} = \sum_{k=1}^{N}C_{i,j+k}^{(n)}(j)(*)_{i,j+k} \tag{45}$$

$$\Xi_x^1\Xi_s^{(n-1)}(*) = \sum_{k=1}^{N}C_{i+k,j}(i)\sum_{k=1}^{N}C_{i,k+j}^{(n-1)}(j)(*)_{i,k+j} \tag{46}$$

$$\Xi_x^{(n-1)}\Xi_s^1(*) = \frac{\partial^{(n)}(*)}{\partial x^{(n-1)}\partial s} = \sum_{k=1}^{N}C_{i+k,j}^{(n-1)}(j)\sum_{k=1}^{N}C_{i+k,j}^{(1)}(i)(*)_{i,k+j} \tag{47}$$

After discretization, the related equations in DQM form are as follows

$$^{DQ}L_{11}\cdot U + {}^{DQ}L_{12}\cdot V + {}^{DQ}L_{13}\cdot W + {}^{DQ}L_{14}\cdot\Phi_x + {}^{DQ}L_{15}\cdot\Phi_y - \rho h\cdot\omega^2 = 0$$
$$^{DQ}L_{21}\cdot U + {}^{DQ}L_{22}\cdot V + {}^{DQ}L_{23}\cdot W + {}^{DQ}L_{24}\cdot\Phi_x + {}^{DQ}L_{25}\cdot\Phi_y - \rho h\cdot\omega^2 = 0$$
$$^{DQ}L_{31}\cdot U + {}^{DQ}L_{32}\cdot V + {}^{DQ}L_{33}\cdot W + {}^{DQ}L_{34}\cdot\Phi_x + {}^{DQ}L_{35}\cdot\Phi_y - \rho h\cdot\omega^2 = 0 \tag{48}$$
$$^{DQ}L_{41}\cdot U + {}^{DQ}L_{42}\cdot V + {}^{DQ}L_{43}\cdot W + {}^{DQ}L_{44}\cdot\Phi_x + {}^{DQ}L_{45}\cdot\Phi_y - \rho h^3\cdot\omega^2/12 = 0$$
$$^{DQ}L_{51}\cdot U + {}^{DQ}L_{52}\cdot V + {}^{DQ}L_{53}\cdot W + {}^{DQ}L_{54}\cdot\Phi_x + {}^{DQ}L_{55}\cdot\Phi_y - \rho h^3\cdot\omega^2/12 = 0$$

The following boundary conditions are used

Simply supported edge (S)

$$V=0,\ W=0,\ N_x=0,\ M_x=0,\ \Psi_s=0=0 \tag{49}$$

Clamped edge (C)

$$U=0,\ V=0,\ W=0,\Psi_x=0,\ \Psi_s=0 \tag{50}$$

From the above procedures, one can derive the general form of eigenvalue equation as follows

$$[G]\{X\} = \Omega[B]\{X\} \tag{51}$$

5. Results

In this study, the following material properties are used

$E_1/E_2 = 40$, $G_{12} = G_{13} = 0.6E_{22}$, $G_{12}/E_2 = 0.5$

$\nu_{12} = \nu_{13} = \nu_{23} = 0.25$

All obtained results are listed in Tables 1-4 for laminated composite circular plate. Two different boundary conditions and two different lay-up (45/-45/-45/45) and (30/-30/-30/30) are also considered. Frequency values for laminated (30/-30/-30/30) and (45/-45/-45/45) circular plates with clamped edges (h/R =0.1, E_1/E_2=40) and simply supoorted edges are tabulated in Tables 1-3, respectively. Frequency values for laminated (45/-45/-45/45) circular plates with clamped edges (h/R =0.1, E_1/E_2=40) for different thickness-to-radius ratio are also listed in Table 4.

Several further examples are also solved and results are presented in Tables 5-10. For comparison purpose, frequency values of laminated (0/60/0) circular plates with clamped edges (a/h=5) are listed in Table 5. The results obtained by using FEM is also given in Table 5 by Kahare and Mittal (2018, 2016) for comparison. It is shown that the present results are in close agreement with the data given by Kahare and Mittal (2018). Thus, the mesh size of 11×11 is used in the next numerical examples, if otherwise is not mentioned. Other comparisons have also made for angle-ply laminated annular and results have been compared with the results by Viswanathan *et al.* (2013). For this purpose, Kevlar-49/epoxy (KGE) and Graphite Epoxy (AS4/3501-6) (AGE) materials are used and clamped-clamped boundary condition is considered. The obtained results are presented in Table 6. According to this table, it can be said that the results are in excellent agreement with the results of Viswanathan *et al*. (2013).

Table 1 Frequency ($\Omega_1 = \omega R^2\sqrt{\rho/E_2}$) for laminated (30/-30/-30/30) circular plates with clamped edges (h/R =0.1, E_1/E_2=40)

	Present DSC results-FSDT(N_s=9)				
Modes	N_x=9	N_x=11	N_x=13	N_x=15	N_x=17
1	24.1030	24.1028	24.1028	24.1028	24.1028
2	36.2178	36.2175	36.2175	36.2175	36.2175
3	44.1162	44.1159	44.1159	44.1159	44.1159
4	51.2389	51.2384	51.2384	51.2384	51.2384
5	56.4077	56.4072	56.4072	56.4072	56.4072

Table 2 Frequency ($\Omega_1 = \omega R^2\sqrt{\rho/E_2h^2}$) for laminated (45/-45/-45/45) circular plates with simply supported edges (h/R =0.1, E_1/E_2=40)

	Present DQ results-(N_s=9)				
Modes	N_x=9	N_x=11	N_x=13	N_x=15	N_x=17
1	17.8034	17.8032	17.8032	17.8032	17.8032
2	32.1048	32.1045	32.1045	32.1045	32.1045
3	41.1987	41.1985	41.1985	41.1985	41.1985
4	52.0370	52.0366	52.0366	52.0366	52.0366
5	54.1032	54.1028	54.1028	54.1028	54.1028
	Present DSC results-FSDT(N_s=9)				
Modes	N_x=9	N_x=11	N_x=13	N_x=15	N_x=17
1	17.8004	17.8004	17.8004	17.8004	17.8004
2	32.1037	32.1037	32.1037	32.1037	32.1037
3	41.1851	41.1853	41.1853	41.1853	41.1855
4	52.0340	52.0341	52.0341	52.0341	52.0343
5	53.9895	53.9903	53.9903	53.9903	53.9906

It is concluded from the results that the lamination ang les and mode numbers have major effect on frequency. It is seen that for all three modes, the frequency para meter decreases when increasing the thickness-to-radius ratio and increases by the increasing value of mode n umbers.

Frequency values of laminated (0/30/0) circular plates with clamped and simply supported edges are listed in Tables 7 and 8 for different thickness and modes. It can be concluded that as the value of the thickness increased frequency decreased for both of edges. It is also concluded that when the number of modes increased frequency values also increased gradually.

It is apparent from the results given in Tables 9-11 that the frequencies decrease monotonically as lamina angles increase. However, the effect of thickness is significant for circular and annular plate vibration. It is clearly shown from these tables that present DSC method converges very fast as the number of grid points increases. It can be also seen that the present DQ and DSC methods show a very good convergence, and solutions obtained from the DSC method are smaller than those produced from the DQ method.

Table 3 Frequency ($\Omega_1 = \omega R^2\sqrt{\rho/E_2h^2}$) for laminated (45/-45/-45/45) circular plates with clamped edges (h/R =0.1, E_1/E_2=40)

		Present DSC results-FSDT(N_s=9)			
Modes	N_x=9	N_x=11	N_x=13	N_x=15	N_x=17
1	25.1826	25.1826	25.1826	25.1826	25.1826
2	40.1075	40.1073	40.1073	40.1073	40.1073
3	44.0850	44.0845	44.0845	44.0845	44.0845
4	57.8141	57.8137	57.8137	57.8137	57.8137
5	58.0143	58.0136	58.0134	58.0134	58.0134

Table 4 Frequency ($\Omega_1 = \omega R^2\sqrt{\rho/E_2h^2}$) values of laminated (45/-45/-45/45) circular plates with clamped edges (h/R =0.1, E_1/E_2=40) for different thickness

		Present DSC results (N_x=11)			
Mod	h/R	N_s=11	N_s=13	N_s=15	N_s=17
1	0.001	46.7548	46.7548	46.7548	46.7548
	0.1	24.8539	24.8539	24.8539	24.8540
	0.2	15.0283	15.0283	15.0283	15.0284
2	0.001	71.1438	71.1438	71.1438	71.1438
	0.1	40.1047	40.1047	40.1048	40.1051
	0.2	23.2196	23.2196	23.2196	23.2198
3	0.001	111.0485	111.0485	111.0485	111.0485
	0.1	44.1173	44.1173	44.1173	44.1175
	0.2	24.6046	24.6046	24.6046	24.6050

Table 5 Comparison of frequency ($\Omega = \omega a^2 \sqrt{\rho h / D}$) values of laminated (0/60/0) circular plates with clamped edges (a/h=5)

Mod	Khare and Mittal (2018)	Present DSC			
		9×11	11×11	13×13	15×13
1	6.6274	6.6402	6.6329	6.6329	6.6329
2	11.4553	11.4652	11.4639	11.4639	11.4639
3	13.2233	13.2515	13.2504	13.2504	13.2504
4	17.3143	17.3304	17.3293	17.3293	17.3293
5	18.2985	18.3125	18.3117	18.3117	18.3117
6	21.5902	21.6192	21.6185	21.6185	21.6185

Table 6 Comparison of frequency values of laminated annular plates (30/-30/30/-30) with C-C edges

Modes	Viswanathan *et al.* (2013)	Present DSC results (N_s=9)			
		N_x=9	N_x=11	N_x=13	N_x=17
1	0.26977	0.2706	0.2703	0.2703	0.2703
2	0.689585	0.6918	0.6911	0.6911	0.6911
3	1.246933	1.2480	1.2473	1.2473	1.2473

Table 7 Frequency ($\Omega = \omega a^2 \sqrt{\rho h / D}$) values of laminated (0/30/0) circular plates with clamped edges

h/a	Modes	Present DSC			
		9×11	13×11	13×13	15×13
0.2	1	6.5298	6.5294	6.5294	6.5294
	2	10.7335	10.7328	10.7328	10.7328
	3	13.5211	13.5207	13.5207	13.5207
	4	17.0040	17.0034	17.0034	17.0034
	5	18.1031	18.1025	18.1025	18.1025
	6	22.0074	22.0053	22.0051	22.0051

	Modes	Present DSC			
		11×11	13×11	13×13	15×13
0.1	1	7.3298	7.3295	7.3295	7.3295
	2	12.8911	12.8903	12.8903	12.8903
	3	16.4645	16.4637	16.4637	16.4637
	4	20.7156	20.7149	20.7149	20.7149
	5	22.7408	22.7397	22.7397	22.7397
	6	29.2314	29.2305	29.2303	29.2303

	Modes	Present DSC			
		11×11	13×11	13×13	15×13
0.05	1	7.5891	7.5891	7.5891	7.5891
	2	13.7251	13.7247	13.7247	13.7247
	3	17.6043	17.6033	17.6033	17.6033
	4	22.7068	22.7056	22.7056	22.7056
	5	24.9377	24.9371	24.9369	24.9369
	6	33.0880	33.0864	33.0861	33.0861

Table 8 Frequency ($\Omega = \omega a^2 \sqrt{\rho h / D}$) values of laminated (0/30/0) circular plates with simply supported edges

h/a	Modes	Present DSC			
		9×11	13×11	13×13	15×13
0.2	1	3.6424	3.6417	3.6417	3.6417
	2	7.8019	7.8012	7.8012	7.8012
	3	10.3705	10.3689	10.3689	10.3689
	4	13.6158	13.6146	13.6146	13.6146
	5	14.9583	14.9571	14.9571	14.9571
	6	17.3121	17.3108	17.3108	17.3108

	Modes	Present DSC			
		9×11	13×11	13×13	15×13
0.1	1	3.8011	3.8004	3.8004	3.8004
	2	8.7450	8.7442	8.7442	8.7442
	3	11.5351	11.5339	11.5339	11.5339
	4	16.0558	16.0547	16.0547	16.0547
	5	17.5911	17.5883	17.5883	17.5883
	6	23.4708	23.4691	23.4691	23.4691

	Modes	Present DSC			
		9×11	13×11	13×13	15×13
0.05	1	3.8269	3.8265	3.8265	3.8265
	2	9.0134	9.0127	9.0127	9.0127
	3	12.0341	12.0329	12.0329	12.0329
	4	16.9475	16.9467	16.9467	16.9467
	5	18.6019	18.6010	18.6008	18.6008
	6	24.7280	24.7265	24.7263	24.7263

Table 9 Fundamental frequency ($\Omega = \omega a^2\sqrt{\rho h/D}$) of laminated annular plates (b/a=0.1;a/h=5) with S-S edges

Lamina scheme	Khare and Mittal (2018)	Present DSC			
		9×11	11×11	13×13	15×13
0/15/0	10.0299	10.0675	10.0660	10.0657	10.0657
0/30/0	9.8554	9.8694	9.8687	9.8683	9.8683
0/45/0	9.6677	9.6848	9.6836	9.6832	9.6832
0/60/0	9.5606	9.5736	9.5728	9.5725	9.5725
0/75/0	9.5485	9.5580	9.5573	9.5569	9.5569

Table 10 Fundamental frequency ($\Omega = \omega a^2\sqrt{\rho h/D}$) of laminated annular plates (b/a=0.5) with C-C edges

a/h	Lamina scheme	Present DSC results				
		9×11	11×11	13×11	13×13	15×13
5	0/15/0	35.1020	35.1018	35.1009	35.1009	35.1009
	0/30/0	34.6868	34.6857	34.6857	34.6857	34.6857
	0/45/0	33.9338	33.9334	33.9325	33.9325	33.9325
	0/60/0	33.5375	33.5371	33.5362	33.5362	33.5362
	Lamina scheme	Present DSC results				
		9×11	11×11	13×11	13×13	15×13
10	0/15/0	57.0262	57.0254	57.0250	57.0250	57.0250
	0/30/0	56.0035	56.0030	56.0028	56.0028	56.0028
	0/45/0	54.8942	54.8934	54.8931	54.8931	54.8931
	0/60/0	53.8175	53.8172	53.8168	53.8167	53.8167
	Lamina scheme	Present DSC results				
		9×11	11×11	13×11	13×13	15×13
20	0/15/0	76.0491	76.0482	76.0482	76.0482	76.0482
	0/30/0	73.6420	73.6417	73.6410	73.6409	73.6409
	0/45/0	71.6643	71.6635	71.6634	71.6634	71.6634
	0/60/0	70.2846	70.2834	70.2831	70.2831	70.2831

Furthermore, some detailed performance of the present DSC method based on two different kernels, some further convergence analyses are also made and accuracy of the two different kernels is examined for laminated plate. For this, the method of DSC based on the two different kernels, FEM (Civalek 1998), and DQM are performed. It is also known (Wei 2000, Wei 2001) that the range of some parameters arises in comparing the numerical efficiency of DSC method such as r, N and kernel types and some of them can be significant for some ranges. In this study, three different error measures are taken into consideration to evaluate the accuracy and convergence of the kernels and quality of the present transformation rules via DSC method. These are as follows

$$L_1 = \frac{1}{(N+1)^2}\sum_{i=0}^{N}\sum_{j=0}^{N}\left|S_{ij} - \bar{S}_{ij}\right| \tag{52}$$

$$L_2 = \frac{1}{(N+1)^2}\sqrt{\sum_{i=0}^{N}\sum_{j=0}^{N}\left|S_{ij} - \bar{S}_{ij}\right|^2} \tag{53}$$

$$E_r = \left|\frac{S_{ij} - \bar{S}_{ij}}{\bar{S}_{ij}}\right| \tag{54}$$

Table 11 Fundamental frequency ($\Omega = \omega a^2 \sqrt{\rho / E_2 h^2}$) of laminated circular plates (h/a=0.1) with clamped edge

Lamina scheme	Present DSC (Regularized Shannon's delta-RSD kernel)				
	9×9	11×11	13×11	13×13	15×13
0/-0/-0/0	23.0193	23.0161	23.0158	23.0158	23.0158
15/-15/-15/15	24.5801	24.5748	24.5739	24.5739	24.5739
30/-30/-30/30	25.5076	25.5066	25.5063	25.5063	25.5063
45/-45/-45/45	25.0095	25.0084	25.0081	25.0081	25.0081
Lamina scheme	Present DSC Lagrange delta sequence-LDS kernel				
	9×9	11×11	13×11	13×13	15×13
0/-0/-0/0	23.1156	23.1073	23.1076	23.1073	23.1073
15/-15/-15/15	24.5968	24.5867	24.5871	24.5867	24.5867
30/-30/-30/30	25.5231	25.5135	25.5135	25.5135	25.5135
45/-45/-45/45	25.0213	25.02446	25.02450	25.02446	25.02446
Lamina scheme	Present DQ				
	9×9	11×11	13×11	13×13	15×13
0/-0/-0/0	23.0261	23.0243	23.0243	23.0243	23.0243
15/-15/-15/15	24.6023	24.6012	24.6012	24.6012	24.6012
30/-30/-30/30	25.5108	25.5094	25.5094	25.5094	25.5094
45/-45/-45/45	25.0120	25.0112	25.0107	25.0107	25.0107

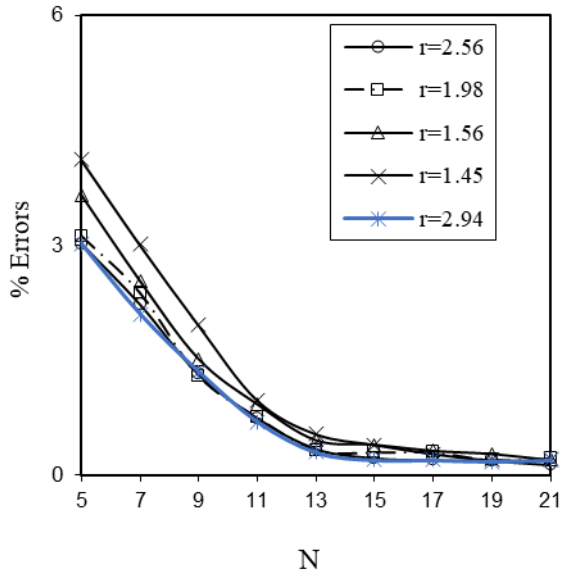

Fig. 2 Convergence and accuracy of clamped annular laminated (30/-30/30/-30) plates for 6th mode frequency (Lagrange delta sequence-LDS kernel) with grid numbers

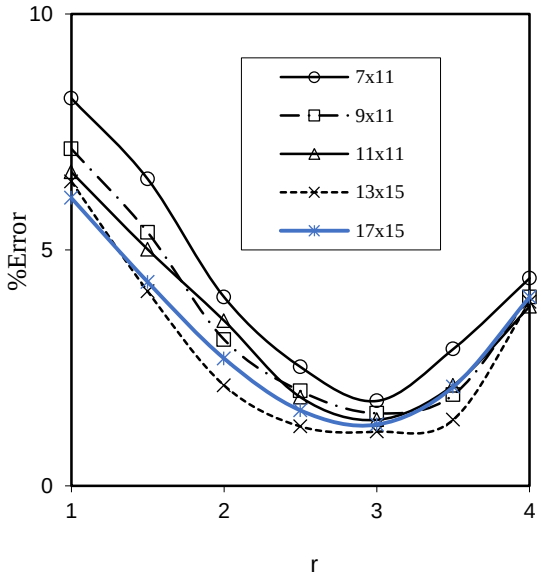

Fig. 3 Convergence of simply supported circular laminated (45/-45/45/-45) plates for 7th mode frequency (Shannon kernel) with DSC regularization

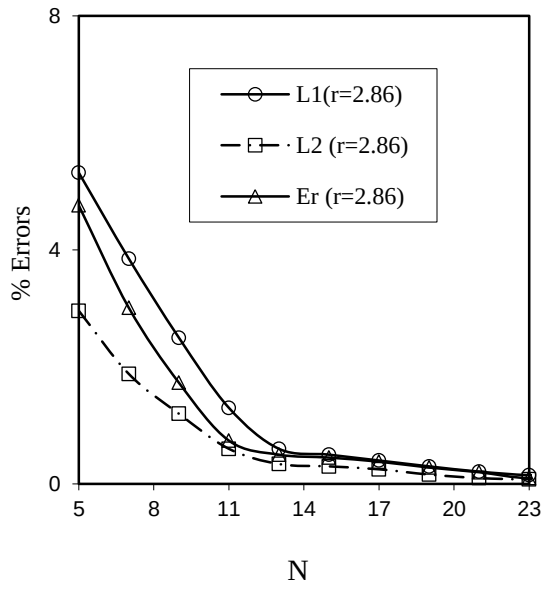

Fig. 4 Error analysis of clamped annular laminated (30/-30/30/-30) plates for 6th mode frequency (Regularized Shannon's delta-RSD kernel; r=2.86)

where S_{ij} and $\bar{S}_{ij}$ are the results calculated by DSC method via different kernels and exact/analytic or reference solution and E_r denotes the relative errors.

Firstly, the errors for 6th frequency values of S-S annular plate with angle-ply laminated scheme with respect to the results given by Viswanathan *et al*. (2013) are figured in Figs. 2 and 3, respectively for two different kernels. It is shown from these figures that the results are efficient for N=11 in each direction. Also, results are very good for Regularized Shannon's delta (RSD) and $2.3<r=\sigma/\Delta<3.1$ parameter. In order to evaluate these parameters, the errors of the solution can be given as the three norms and are

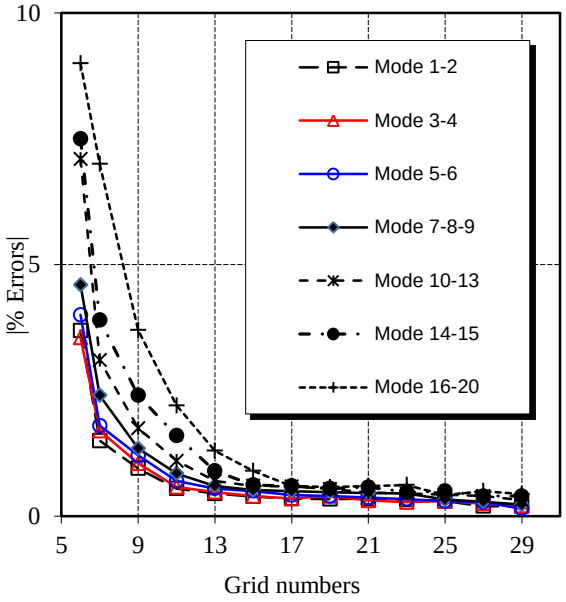

Fig. 5 Convergence of laminated annular plates for different modes with clamped edges with different grid numbers (Regularized Shannon's delta-RSD kernel)

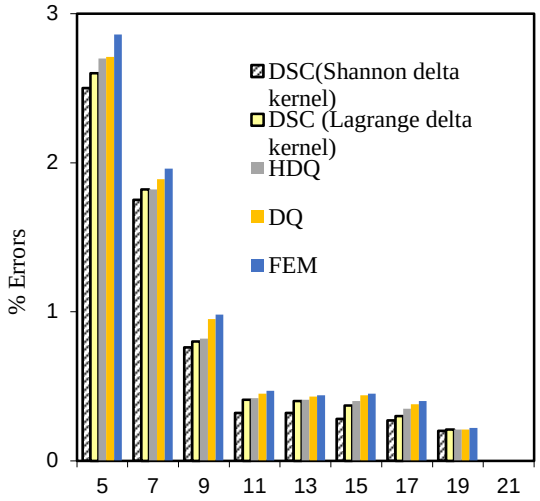

Fig. 6 Error analysis of angle-play laminated circular plates for 9th mode frequency with simply supported edges with different grid numbers

illustrated in Fig. 4. Also, in Figs. 5 and 6, convergence is tested for different modes and methods. It is found that as the grid numbers increase the percentage error also decreases. For DSC regularized parameter, r, DSC method provides acceptable results with a maximum discrepancy of 1.15% for r=2.86 and N=11. Namely, a biggest value r is required, to obtain the convergence for higher frequency component of errors function. However, for N=15, this error is reduced to 0.70% for same regularized parameter. So, the DSC parameters can be more suitable as N=15 and σ/Δ = 2.86 using Regularized Shannon's delta (RSD) kernel. It is also shown from these figures that only 11 grid points can yield accurate results for frequency in lower modes. However, in higher modes, the method of DSC requires 13 grids in each direction for accurate results. In order to compare with other methods and to test the performance of the DSC method, clamped annular laminated plate vibration problem (Viswanathan *et al*. (2013) is selected and solved by three different methods. It is shown that DSC results using 13 grid points are more accurate than harmonic differential quadrature (HDQ) and FE methods for higher modes. A reasonably converged solution may be achieved for 15 grids by FEM. In addition to this, a reasonably converged solution may be obtained for 13 grid points using HDQ.

6. Conclusions

Frequency analyses of composite laminated circular plates are examined by DQ and DSC methods. FSDT shell theory is used for modeling of laminated circular plates. Effects of different angle/lamination on frequency values of laminated plates are investigated. The previous studies showed that Shannon's delta kernel gives the best result. Also, DSC is more suitable for higher modes (first 30 modes are obtained) even not reported in this study. Governing equations of motion of circular plates are reduced by the conical shell equations of motion. For computational calculation, two numerical methods are applied. It is concluded from the results that two methods have very good convergence. It is also concluded that the method of discrete singular convolution (DSC) based on Shannon's delta kernel is a promising and potential approach for computational mechanics of composite plates for free vibration of higher modes.

Acknowledgements

This work was partially supported by the Research Center for Interneural Computing of China Medical University of Taiwan. Ö mer Civalek would like to thank the committee member of Research Center for Interneural Computing of China Medical University of Taiwan for their help during solution of some mathematical equations.

References

Abdelaziz, H.H., Meziane, M.A.A., Bousahla, A.A., Tounsi, A., Mahmoud, S.R. and Alwabli, A.S. (2017), "An efficient hyperbolic shear deformation theory for bending, buckling and free vibration of FGM sandwich plates with various boundary conditions", *Steel Compos. Struct*., **25**(6), 693-704. https://doi.org/10.12989/scs.2017.25.6.693

Akgoz, B. and Civalek, O. (2012), "Analysis of micro-sized beams for various boundary conditions based on the strain gradient elasticity theory", *Arch. Appl. Mech*. **82**, 423-443. https://doi.org/10.1007/s00419-011-0565-5

Akgoz, B. and Civalek, O. (2017), "Effects of thermal and shear deformation on vibration response of functionally graded thick composite microbeams", *Compos. Part B: Eng*, **129**, 77-87. https://doi.org/10.1016/j.compositesb.2017.07.024

Aleksandrova, N.N. (2016), "Effect of thermal gradients on stress/strain distributions in a thin circular symmetric plate", *Struct. Eng. Mech*., **58**(4), 627-639. https://doi.org/10.12989/sem.2016.58.4.627

Arefi, M., Mohammadi, M., Tabatabaeian, A., Dimitri, R. and Tornabene, F. (2018), "Two-dimensional thermo-elastic analysis of FG-CNTRC cylindrical pressure vessels", *Steel Compos. Struct*., **27**(4), 525-536. https://doi.org/10.12989/scs.2018.27.4.525

Avcar, M. (2019), "Free vibration of imperfect sigmoid and power law functionally graded beams", *Steel Compos. Struct.*, **30**(6), 603-615. https://doi.org/10.12989/scs.2019.30.6.603

Avcar, M. (2015), "Effects of rotary inertia shear deformation and non-homogeneity on frequencies of beam", *Struct. Eng. Mech*., **55**(4), 871-884. https://doi.org/10.12989/sem.2015.55.4.871

Azimi, S. (1988), "Free vibration of circular plates with elastic edge supports using the receptance method", *J. Sound Vib*., **120** (1) 19-35. https://doi.org/10.1016/0022-460X(88)90332-X.

Baltacioglu, A.K., Akgoz, B. and Civalek, O. (2010), "Nonlinear static response of laminated composite plates by discrete singular convolution method", *Compos. Struct.*, **93**, 153-161. https://doi.org/10.1016/j.compstruct.2010.06.005.

Baltacioglu, A.K., Civalek, O., Akgoz, B. and Demir, F. (2011), "Large deflection analysis of laminated composite plates resting on nonlinear elastic foundations by the method of discrete singular convolution", *Int. J. Pres. Ves. Pip.*, **88**, 290-300. https://doi.org/10.1016/j.ijpvp.2011.06.004.

Benchohra, M., Driz, H., Bakora, A., Tounsi, A., Bedia, E.A.A. and Mahmoud, S.R. (2018), "A new quasi-3D sinusoidal shear deformation theory for functionally graded plates", *Struct. Eng. Mech.*, **65**(1), 19-31. https://doi.org/10.12989/sem.2018.65.1.019.

Bisadi, H., Eshaghi, M., Rokni, H., *et al.* (2012), "Benchmark solution for transverse vibration of annular Reddy plates", *Int. J. Mech. Sci.*, **56**(1), 35-49. https://doi.org/10.1016/j.ijmecsci.2011.12.007.

Bouchafa, A., Bouiadjra, M.B., Houari, M.S.A. and Tounsi, A. (2015), "Thermal stresses and deflections of functionally graded sandwich plates using a new refined hyperbolic shear deformation theory", *Steel Compos. Struct.*, **18**(6), 1493- 1515. https://doi.org/10.12989/scs.2015.18.6.1493.

Bouderba, B., Houari, M.S.A., Tounsi, A. and Mahmoud, S.R. (2016), "Thermal stability of functionally graded sandwich plates using a simple shear deformation theory", *Struct. Eng. Mech.*, **58**(3), 397-422. https://doi.org/10.12989/sem.2016.58.3.397.

Civalek, O. (2007), "Linear vibration analysis of isotropic conical shells by discrete singular convolution (DSC)", *Struct Eng Mech.*, **25**(1), 127–130. https://doi.org/10.12989/sem.2007.25.1.127.

Civalek, O. (1998), "Finite Element analysis of plates and shells", MSc Dissertation, Fırat University, Elazığ. (in Turkish).

Civalek, O. (2004), "Geometrically non-linear static and dynamic analysis of plates and shells resting on elastic foundation by the method of polynomial differential quadrature (PDQ)", Ph.D. Dissertation, Fırat University, Elazığ. (in Turkish).

Civalek, O. (2006a), "Free vibration analysis of composite conical shells using the discrete singular convolution algorithm", *Steel Compos. Struct.*, **6**(4), 353-366. https://doi.org/10.12989/scs.2006.6.4.353.

Civalek, O. (2006b), "The determination of frequencies of laminated conical shells via the discrete singular convolution method", *J. Mech. Mater. Struct.*, **1**(1), 163-182. http://dx.doi.org/10.2140/jomms.2006.1.163.

Civalek, O. (2008a), "Vibration analysis of conical panels using the method of discrete singular convolution", *Commun. Numer. Meth. Eng.*, **24**, 169-181. https://doi.org/10.1002/cnm.961.

Civalek, O. (2008b), "Analysis of thick rectangular plates with symmetric cross-ply laminates based on first-order shear deformation theory", *J. Compos. Mater.*, **42**, 2853-2867. https://doi.org/10.1177%2F0021998308096952.

Civalek, O. (2013a), "Nonlinear dynamic response of laminated plates resting on nonlinear elastic foundations by the discrete singular convolution-differential quadrature coupled approaches", *Compos. Part B: Eng.*, **50**, 171-179. https://doi.org/10.1016/j.compositesb.2013.01.027.

Civalek, O. (2013b), "Vibration analysis of laminated composite conical shells by the method of discrete singular convolution based on the shear deformation theory", *Compos. Part B: Eng*., **45**(1), 1001-1009. https://doi.org/10.1016/j.compositesb.2012.05.018.

Civalek, O. (2017), "Free vibration of carbon nanotubes reinforced (CNTR) and functionally graded shells and plates based on FSDT via discrete singular convolution method", *Compos. Part*

B: Eng., **111**, 45-59. https://doi.org/10.1016/j.compositesb.2016.11.030.
Civalek, O. and Akgoz, B. (2011), "Nonlinear vibration analysis of laminated plates resting on nonlinear two-parameters elastic foundations", *Steel Compos. Struct.*, **11**(5), 403-421. https://doi.org/10.12989/scs.2011.11.5.403.
Civalek, O. and Acar, M.H. (2007), "Discrete singular convolution method for the analysis of Mindlin plates on elastic foundations", *Int. J. Pres. Ves. Pip.*, **84**, 527-535. https://doi.org/10.1016/j.ijpvp.2007.07.001.
Civalek, O. and Demir, C. (2011), "Bending analysis of microtubules using nonlocal Euler-Bernoulli beam theory", *Appl. Math. Model.*, **35**, 2053-2067. https://doi.org/10.1016/j.apm.2010.11.004.
Civalek, O. and Demir, C. (2016), "A simple mathematical model of microtubules surrounded by an elastic matrix by nonlocal finite element method", *Appl. Math. Comput.*, **289**,335-352. https://doi.org/10.1016/j.amc.2016.05.034.
Civalek, O., Korkmaz, A. and Demir, Ç. (2010), "Discrete singular convolution approach for buckling analysis of rectangular Kirchhoff plates subjected to compressive loads on two opposite edges", *Adv. Eng. Softw.*, **41**, 557-560. https://doi.org/10.1016/j.advengsoft.2009.11.002.
Civalek, O., Mercan, K. and Demir, C. (2016), "Vibration analysis of FG cylindrical shells with power-law index using discrete singular convolution technique", *Curved Layer. Struct.*, **3**, 82-90. https://doi.org/10.1515/cls-2016-0007.
Demir, C. and Civalek, O. (2017), "On the analysis of microbeams", *Int. J. Eng. Sci.*, **121**, 14-33. https://doi.org/10.1016/j.ijengsci.2017.08.016.
Demir, C., Mercan, K. and Civalek, O. (2016), "Determination of critical buckling loads of isotropic, FGM and laminated truncated conical panel", *Compos. Part B Eng.*, **94**, 1-10. https://doi.org/10.1016/j.compositesb.2016.03.031.
Duan, G., Wang, X. and Jin, C. (2014), "Free vibration analysis of circular thin plates with stepped thickness by the DSC element method", *Thin Wall. Struct.*, **85**, 25-33. https://doi.org/10.1016/j.tws.2014.07.010.
Fantuzzi, N. and Tornabene, F. (2014), "Strong formulation finite element method for arbitrarily shaped laminated plates- Part I. Theoretical analysis", *Adv. Aircr. Spacecr. Sci.*, **1**(2), 125-143. http://dx.doi.org/10.12989/aas.2014.1.2.125.
Gürses, M., Akgoz, B. and Civalek, O. (2012), "Mathematical modeling of vibration problem of nano-sized annular sector plates using the nonlocal continuum theory via eight-node discrete singular convolution transformation", *Appl. Math. Comput.*, **219**, 3226-3240. https://doi.org/10.1016/j.amc.2012.09.062.
Gürses, M., Civalek, Ö., Korkmaz, A. and Ersoy, H. (2009), "Free vibration analysis of symmetric laminated skew plates by discrete singular convolution technique based on first-order shear deformation theory", *Int. J. Numer. Method. Eng.*, **79**, 290-313. https://doi.org/10.1002/nme.2553.
Hamzehkolaei, N.S., Malekzadeh, P. and Vaseghi, J. (2011), "Thermal effect on axisymmetric bending of functionally graded circular and annular plates using DQM", *Steel Compos. Struct.*, **11**(4), 341-358. https://doi.org/10.12989/scs.2011.11.4.341.
Hou, Y., Wei, G.W. and Xiang, Y. (2005), "DSC-Ritz method for the free vibration analysis of Mindlin plates", *Int. J. Numer. Meth. Eng.*, **62**, 262-288. https://doi.org/10.1002/nme.1186.
Jhung, M.J., Choi, Y.H. and Kim, H.J. (2005), "Natural vibration characteristics of a clamped circular plate in contact with fluid", *Struct. Eng. Mech.*, **21**(2), 169-184. https://doi.org/10.12989/sem.2005.21.2.169.
Khare, S. and Mittal, N.D. (2016), "Three-dimensional free vibration analysis of thick laminated circular plates", *Int. J. Eng., Sci. Technol.*, **8**(2), 11-29. http://dx.doi.org/10.4314/ijest.v8i2.2.
Khare, S. and Mittal, N.D. (2018), "Free vibration of thick laminated circular and annular plates using three-dimensional finite element analysis", *AEJ - Alexandria Eng. J.*, **57**(3), 1217-1228. https://doi.org/10.1016/j.aej.2017.03.006.
Leissa, A.W. (1993), *Vibration of shells*, Acoustical Society of America, Melville, NY, USA.
Malekzadeh, P. (2009), "Three-dimensional free vibration analysis of thick laminated annular sector plates using a hybrid method", *Compos. Struct.*, **90**, 428–437. https://doi.org/10.1016/j.compstruct.2009.04.015.
Mehditabar, A., Rahimi, G.H. and Fard, K.M. (2018), "Vibrational responses of antisymmetric angle-ply laminated conical shell by the methods of polynomial based differential quadrature and Fourier expansion based differential quadrature", *Appl. Math. Comput.*, **320**, 580-595. https://doi.org/10.1016/j.amc.2017.10.017.
Mercan, K. and Civalek, O. (2016), "DSC method for buckling analysis of boron nitride nanotube (BNNT) surrounded by an elastic matrix", *Compos. Struct.*, **143**, 300-309. https://doi.org/10.1016/j.compstruct.2016.02.040.
Mercan, K. and Civalek, O. (2017), "Buckling analysis of Silicon carbide nanotubes (SiCNTs) with surface effect and nonlocal elasticity using the method of HDQ", *Compos. Part B: Eng.*, **114**, 34-45. https://doi.org/10.1016/j.compositesb.2017.01.067.
Pang, F., Li, H., Miao, X. and Wang, X. (2017), "A modified Fourier solution for vibration analysis of moderately thick laminated annular sector plates with general boundary conditions, internal radial line and circumferential arc supports", *Curved Layer. Struct.*, **4**, 189-220. https://doi.org/10.1515/cls-2017-0014.
Qatu, M. (2004), *Vibration Of Laminated Shells And Plates*, Academic Press, U.K.
Reddy, J.N. (2003), *Mechanics Of Laminated Composite Plates And Shells: Theory And Analysis*, (2nd edition), CRC Press, New York, NY, USA.
Saidi, A.R., Baferani, A.H. and Jomehzadeh, E. (2011), "Benchmark solution for free vibration of functionally graded moderately thick annular sector plates", *Acta Mech.*, **219**, 309-335. https://doi.org/10.1007/s00707-011-0459-1.
Sharma, A., Sharda, H.B. and Nath, Y. (2005), "Stability and vibration of thick laminated composite sector plates", *J. Sound Vib.*, **287**, 1-23. https://doi.org/10.1016/j.jsv.2004.10.030.
Shu, C. and Xue, H. (1997), "Explicit computations of weighting coefficients in the harmonic differential quadrature", *J. Sound Vib.*, **204**(3), 549-555. https://doi.org/10.1006/jsvi.1996.0894.
Soedel, W. (2004), *Vibrations of shells and plates*, (3rd edition), CRC Press, New York, NY, USA.
Striz, A.G., Wang, X. and Bert, C.W. (1995), "Harmonic differential quadrature method and applications to analysis of structural components", *Acta Mech.*, **111**, 85-94. https://doi.org/10.1007/BF01187729.
Su, Z., Jin, G. and Wang X. (2015), "Free vibration analysis of laminated composite and functionally graded sector plates with general boundary conditions", *Compos. Struct.*, **132**, 720-736. https://doi.org/10.1016/j.compstruct.2015.06.008.
Su, Z., Jin, G. and Ye, T. (2014), "Three-dimensional vibration analysis of thick functionally graded conical, cylindrical shell and annular plate structures with arbitrary elastic restraints", *Compos. Struct.*, **118**, 432-447. https://doi.org/10.1016/j.compstruct.2014.07.049
Tahouneh, V. (2014), "Free vibration analysis of bidirectional functionally graded annular plates resting on elastic foundations using differential quadrature method", *Struct. Eng. Mech.*, **52**(4), 663-686. https://doi.org/10.12989/sem.2014.52.4.663
Tornabene, F. and Fantuzzi, N. (2014), *Mechanics of laminated*

composite doubly-curved shell structures, the generalized differential quadrature method and the strong formulation finite element method. Società Editrice Esculapio, Bologna, Italy.

Tornabene, F., Fantuzzi, N. and Bacciocchi, M. (2014), "The local GDQ method applied to general higher-order theories of doubly-curved laminated composite shells and panels: the free vibration analysis", *Compos. Struct.*, **116**, 637-660. https://doi.org/10.1016/j.compstruct.2014.05.008

Tornabene, F., Fantuzzi, N., Bacciocchi, M. and Viola, E. (2016), "Effect of agglomeration on the natural frequencies of functionally graded carbon nanotube-reinforced laminated composite doubly-curved shells", *Compos. Part B: Eng.*, **89**, 187-218. https://doi.org/10.1016/j.compositesb.2015.11.016.

Tornabene, F., Fantuzzi, N., Viola, E. and Ferreira, A.J.M. (2013), "Radial basis function method applied to doubly-curved laminated composite shells and panels with a General Higher-order Equivalent Single Layer formulation", *Compos. Part B: Eng.*, **55**, 642-659. https://doi.org/10.1016/j.compositesb.2013.07.026.

Viswanathan, K.K. and Sheen, D. (2009), "Free vibration of layered annular circular plate of variable thickness using spline function approximation", *Indian J. Eng. Mater. Sci*., **16**, 433-448.

Viswanathan, K.K., Javed, S., Prabakar, K., Aziz, Z.A. and Bakar, I.A. (2015), "Free vibration of anti-symmetric angle-ply laminated conical shells", *Compos. Struct.*, **122**, 488-495. https://doi.org/10.1016/j.compstruct.2014.11.075.

Viswanathan, K.K., Javed, S. and Zainal A.A. (2013), "Free vibration of antisymmetric angle-ply laminated annular circular pplate", *Proceedings of the World Congress on Engineering*, Vol III, WCE 2013, July 3 - 5, London.

Wang, Q., *et al.* (2016b), "A unified solution for free in-plane vibration of orthotropic circular, annular and sector plates with general boundary conditions", *Appl. Math. Model.*, **40**(21), 9228-9253. https://doi.org/10.1016/j.apm.2016.06.005.

Wang, Q., Shi, D., Liang, Q. and Ahad, F. (2016a), "An improved Fourier series solution for the dynamic analysis of laminated composite annular, circular, and sector plate with general boundary conditions", *J. Comp. Mater.*, **50**(30), 4199-4233. https://doi.org/10.1177%2F0021998316635240.

Wang, X., Wang, Y. and Xu, S. (2012), "DSC analysis of a simply supported anisotropic rectangular plate", *Compos. Struct.*, **94**, 2576-2584. https://doi.org/10.1016/j.compstruct.2012.03.005.

Wei, G.W. (2001a), "Vibration analysis by discrete singular convolution", *J. Sound Vib.*, **244**, 535-553. https://doi.org/10.1006/jsvi.2000.3507.

Wei, G.W. (2001b), "Discrete singular convolution for beam analysis", *Eng. Struct.*, **23**, 1045-1053. https://doi.org/10.1016/S0141-0296(01)00016-5.

Wei, G.W., Zhao, Y.B. and Xiang, Y. (2001), "The determination of natural frequencies of rectangular plates with mixed boundary conditions by discrete singular convolution" *Int. J. Mech. Sci.*, **43**, 1731-1746. https://doi.org/10.1016/S0020-7403(01)00021-2.

Wei, G.W., Zhao, Y.B. and Xiang, Y. (2002a), "A novel approach for the analysis of high-frequency vibrations", *J. Sound Vib.*, **257**, 207-246. https://doi.org/10.1006/jsvi.2002.5055.

Wei, G.W., Zhao, Y.B. and Xiang, Y. (2002b),"Discrete singular convolution and its application to the analysis of plates with internal supports. Part 1: Theory and algorithm", *Int. J. Numer. Meth. Eng.*, **55**, 913-946. https://doi.org/10.1002/nme.526.

Wu, C.P. and Yu, L.T. (2016), "A state space meshless method for the 3D analysis of FGM axisymmetric circular plates", *Steel Compos. Struct.*, **22**(1), 161-182. https://doi.org/10.12989/scs.2016.22.1.161

Wu, C.P. and Yu, L.T., (2018), "Quasi-3D static analysis of two-directional functionally graded circular plates", *Steel Compos Struct.*, **27**(6), 789-801. https://doi.org/10.12989/scs.2018.27.6.789

Yousefzadeh, Sh., Jafari, A.A., Mohammadzadeh, A., *et al.* (2018), "Dynamic response of functionally graded annular/circular plate in contact with bounded fluid under harmonic load", *Struct. Eng. Mech*., **65**(5), 523-533. https://doi.org/10.12989/sem.2018.65.5.523

CC

Appendix

The related differential operators are as follows

$$L_{11} = A_{11}\cdot U_{,xx} + \frac{A_{11}}{R(x)}\cdot \sin\alpha\cdot U_{,x} - \frac{A_{22}}{R^2(x)}\cdot U\cdot \sin^2\alpha + \frac{A_{33}}{R^2(x)}\cdot U_{,ss}$$

$$L_{12} = \frac{(A_{12}+A_{33})}{R(x)}\cdot \sin\alpha\cdot V_{,xs} - \frac{(A_{22}+A_{33})}{R^2(x)}\cdot \sin\alpha\cdot V_{,s}$$

$$L_{13} = \frac{A_{12}}{R(x)}\cos\alpha\cdot W_{,x} - \frac{A_{22}}{R^2(x)}\cdot W\cdot \sin\alpha\cdot\cos\alpha$$

$$L_{14} = B_{11}\cdot \Phi_{x,xx} + \frac{B_{11}}{R(x)}\cdot \sin\alpha\cdot \Phi_{x,x} - \frac{B_{22}}{R^2(x)}\cdot \Phi_{x}\cdot \sin^2\alpha + \frac{B_{33}}{R^2(x)}\cdot \Phi_{x,ss}$$

$$L_{15} = \frac{(B_{12}+B_{33})}{R(x)}\cdot \Phi_{s,xs} - \frac{(B_{22}+B_{33})}{R^2(x)}\cdot \sin\alpha\cdot \Phi_{s,s}$$

$$L_{21} = \frac{(A_{12}+A_{33})}{R(x)}\cdot U_{,xs} + \frac{(A_{22}+A_{33})}{R^2(x)}\cdot \sin\alpha\cdot U_{,s}$$

$$L_{22} = A_{33}\cdot V_{,xx} + A_{33}\frac{\sin\alpha}{R(x)}\cdot V_{,x}$$

$$-\frac{A_{33}}{R^2(x)}\cdot V\cdot \sin^2\alpha + \frac{A_{22}}{R^2(x)}\cdot V_{,ss} - \frac{A_{44}}{R^2(x)}\cdot V\cdot \cos^2\alpha$$

$$L_{23} = \frac{(A_{22}+A_{44})}{R^2(x)}\cdot \cos\alpha\cdot W_{,s}$$

$$L_{24} = \frac{(B_{12}+B_{33})}{R(x)}\cdot \Psi_{x,xs} + \frac{(B_{22}+B_{33})}{R^2(x)}\cdot \sin\alpha\cdot \Psi_{x,s}$$

$$L_{25} = B_{33}\cdot \Psi_{s,xx} + B_{33}\cdot \frac{1}{R(x)}\cdot \sin\alpha\cdot \Psi_{s,x}$$

$$-B_{33}\cdot \frac{1}{R^2(x)}\cdot \Psi_{s}\cdot \sin^2\alpha + B_{22}\frac{1}{R^2(x)}\cdot \Psi_{s,ss} + A_{44}\cdot \frac{1}{R(x)}\cdot \Psi_{s}\cdot \cos\alpha$$

$$L_{31} = -A_{12}\frac{1}{R(x)}\cdot \cos\alpha\cdot U_{,x} - A_{22}\cdot \frac{1}{R^2(x)}\cdot U\cdot \sin\alpha\cdot\cos\alpha$$

$$L_{32} = -\frac{(A_{22}+A_{44})}{R^2(x)}\cdot \cos\alpha\cdot V_{,s}$$

$$L_{33} = A_{55}\cdot W_{,xx} + A_{55}\frac{1}{R(x)}\cdot \sin\alpha\cdot W_{,s}$$

$$+ A_{44}\cdot \frac{1}{R^2(x)}\cdot W_{,ss} - A_{22}\cdot \frac{1}{R^2(x)}\cdot W\cdot \cos^2\alpha$$

$$L_{34} = A_{55}\cdot \Psi_{x,x} - B_{12}\cdot \frac{1}{R(x)}\cdot \cos\alpha\cdot \Psi_{x,x}$$

$$+ A_{55}\cdot \frac{1}{R(x)}\cdot \Psi_{x}\cdot \sin\alpha - B_{22}\cdot \frac{1}{R^2(x)}\cdot \Psi_{x}\cdot \sin\alpha\cdot\cos\alpha$$

$$L_{35} = A_{44}\cdot \frac{1}{R(x)}\cdot \Psi_{s,s} - B_{22}\cdot \frac{1}{R^2(x)}\cdot \cos\alpha\cdot \Psi_{s,s}$$

$$L_{41} = B_{11}\cdot U_{,xx} + \frac{B_{11}}{R(x)}\cdot \sin\alpha\cdot U_{,x} - \frac{B_{22}}{R^2(x)}\cdot U\cdot \sin^2\alpha + \frac{B_{33}}{R^2(x)}\cdot U_{ss}$$

$$L_{42} = \frac{(B_{12}+B_{33})}{R(x)}\cdot V_{,xs} - \frac{(B_{22}+B_{33})}{R^2(x)}\cdot \sin\alpha\cdot V_{,s}$$

$$L_{43} = -A_{55}\cdot W_{,x} + B_{12}\cdot \frac{\cos\alpha}{R(x)}\cdot W_{,x} - \frac{B_{22}}{R^2(x)}\cdot W\cdot \sin\alpha\cdot\cos\alpha$$

$$L_{44} = D_{11}\cdot \Psi_{x,xx} + D_{11}\cdot \frac{\sin\alpha}{R(x)}\cdot \Psi_{x,x} - \frac{D_{22}}{R^2(x)}\cdot \Psi_{x}\cdot \sin^2\alpha$$

$$+ \frac{D_{33}}{R^2(x)}\cdot \Psi_{x,ss} - A_{55}\cdot \Psi_{x}$$

$$L_{45} = \frac{(D_{12}+D_{33})}{R(x)}\cdot \Psi_{s,xs} - \frac{(D_{22}+D_{33})}{R^2(x)}\cdot \Psi_{s,s}\cdot \sin\alpha$$

$$L_{51} = \frac{(B_{12}+B_{33})}{R(x)}\cdot U_{,xs} + \frac{(B_{22}+B_{33})}{R^2(x)}\cdot U_{,s}\cdot \sin\alpha$$

$$L_{52} = B_{33}\cdot V_{,xx} + B_{33}\frac{\sin\alpha}{R(x)}\cdot V_{,x}$$

$$-B_{33}\cdot \frac{\sin^2\alpha}{R^2(x)}\cdot V + \frac{B_{22}}{R^2(x)}\cdot V_{,ss} + \frac{A_{44}}{R(x)}\cdot V\cdot \cos\alpha$$

$$L_{53} = -\frac{A_{44}}{R(x)}\cdot W_{,s} + \frac{B_{22}}{R^2(x)}\cdot \cos\alpha\cdot W_{,s}$$

$$L_{54} = \frac{(D_{12}+D_{33})}{R(x)}\cdot \Psi_{x,xs} + \frac{(D_{22}+D_{33})}{R^2(x)}\cdot \sin\alpha\cdot \Psi_{x,s}$$

$$L_{55} = D_{33}\cdot \Psi_{s,xs} + D_{33}\cdot \frac{\sin\alpha}{R(x)}\cdot \Psi_{s} - \frac{D_{33}}{R^2(x)}\cdot \Psi_{s,x}\cdot \sin^2\alpha$$

$$+ \frac{D_{22}}{R^2(x)}\cdot \Psi_{s,ss} - A_{44}\cdot \Psi_{s}$$